

Phthalocyanoruthenium complexes and polymers with bridged ligands

Fernando Mendizabal*

Departamento de Química, Facultad de Ciencias, Universidad de Chile, Casilla 653- Santiago, Chile

Received 26 July 2001; accepted 21 August 2001

Abstract

Electronic properties related to the semiconductivity of monomers and polymers of phthalocyanoruthenium with bidentate bridging ligands, $[\text{PcRu}(\text{L}_2)]$ and $[\text{PcRu}(\text{L})]_n$, have been investigated from density functional calculations ($\text{L} = \text{pyrazine}$, triazine, tetrazine, 4,4'-bipyridine, and bipyridylacetylene). The Pauli repulsion is the origin that the bridging axial ligands (L) prefer be located towards the aza positions of the macrocycle. The intrinsic semiconducting properties depend on the frontier band. The valence band is composed largely by the ruthenium d_{xy} orbital. The conduction band is composed for a mixture between the metallomacrocycle and bridged ligand orbitals for systems formed by pyrazine, bipyridine, and bipyridylacetylene. However, this composition is different when the ligands are triazine and tetrazine, which they show a band composed by π^* orbitals. © 2002 Elsevier Science B.V. All rights reserved.

Keywords: Phthalocyaninoruthenium complexes and polymers; Electronic properties; Density functional calculations

1. Introduction

Monomeric and bridged biaxially coordinated transition-metal complexes $[\text{MacM}(\text{L}_2)]$ and polymers $[\text{MacM}(\text{L})]$ with phthalocyanine (Pc) and tetrabenzoporphyrine (TBP) as the macrocycles (Mac), transition metals, e.g. Fe, Ru, Os, or Co, as the central metal atom (M), and bidentate ligands (L), e.g. pyrazine (pyz), triazine (tri), tetrazine (tz), 4,4'-bipyridine (bpy), and bipyridylacetylene (bpyac), have been investigated experimentally [1–10] and theoretically [11–15] for their semiconducting properties. They have been classified as 'shish-kebab polymers' [1].

The electrical properties exhibited by these systems have attracted much attention [16–18]. For instance,

the bridged transition metal compounds are fairly stable polymers that exhibit intrinsic conductivities, without external oxidative doping. These polymers show a technological interest due to their comparatively high thermal stability and good semiconducting properties [19–21]. The experimental band gaps values varied between 0.1 and 1.5 eV, which define them as semiconductors [22–25]. One of the factors responsible for the electrical conductivity in these complexes is the band gap, which may be approximated as the energy difference between the LUMO and HOMO states [13–15].

Theoretical studies based on density functional theory and Hückel Extended on polymers $[\text{PcFe}(\text{L})]_n$ ($\text{L} = \text{pyz}$, tri, tz, bpy, bpyac) showed that the intrinsic semiconducting properties depend on the frontier band [13,15]. The valence band is composed largely by the transition metal d_{xy} orbital. The conduction

* Tel.: +56-2-678-7397; fax: +56-2-271-3888.

E-mail address: hagua@abello.dic.uchile.cl (F. Mendizabal).

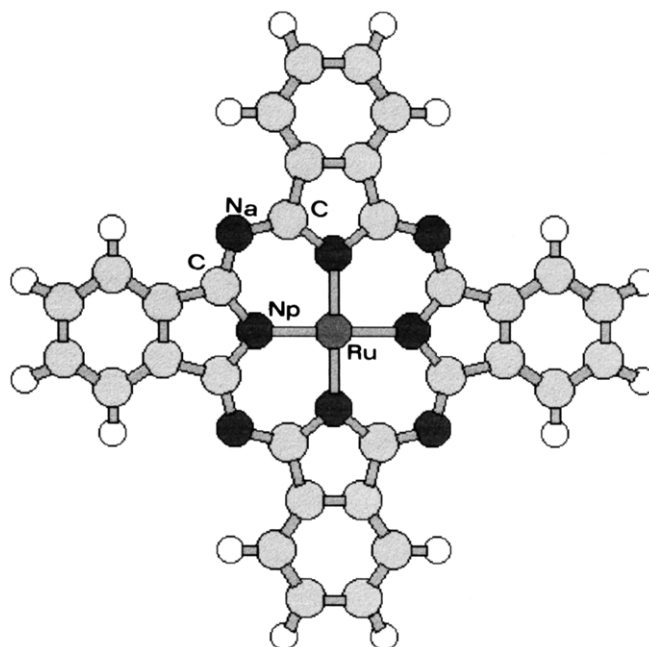


Fig. 1. Phthalocyanoruthenium [PcRu].

band is composed for a mixture between the metallo-macrocycle and bridged ligand orbitals for systems formed by pyrazine, bipyridine, and bipyridylacetylene. However, this composition changes drastically when the ligands are triazine and tetrazine, since such a band is composed thoroughly by π^* orbitals. These systems show the higher conductivity within the series, in agreement with experimental results [16–25].

Therefore, it is of interest in this work to investigate the electronic structure of the ruthenium compounds ($[\text{PcRu}(\text{L})_2]$ and $[\text{PcRu}(\text{L})]_n$) through density functional approach. We will put special emphasis on the study of the metal-bridged ligand interactions. We try to answer some questions concerning the electronic properties of the complexes such as: the location of the plane of the bridged ligand, the nature and the magnitude of the band gap HOMO–LUMO, and

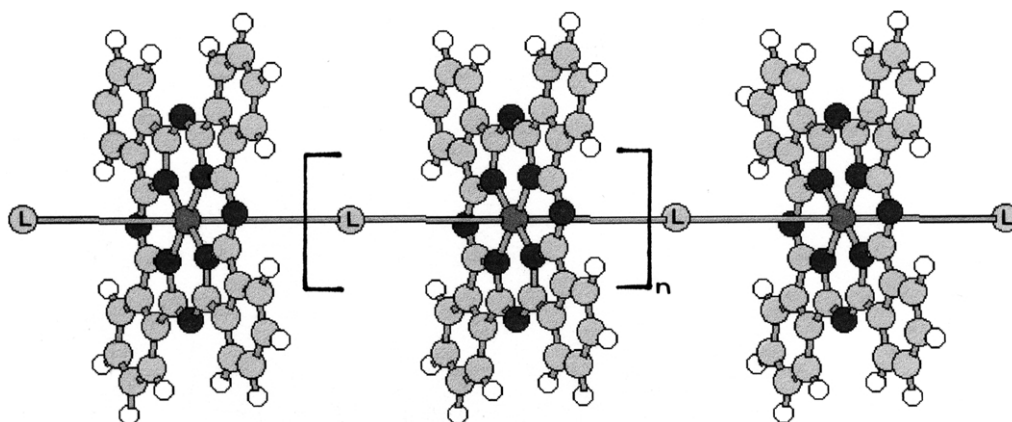


Fig. 2. Structures of the metallo-macrocycle polymers and their related complexes.

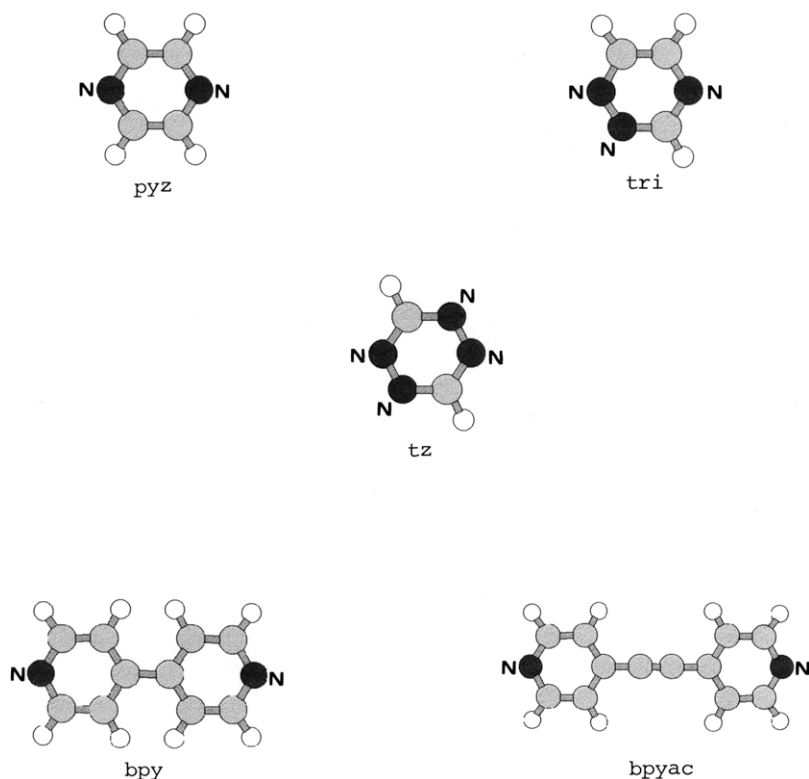


Fig. 3. Bridged ligands (L) pyz, tri, tz, bpy, bpyac.

the relationship between the structural and electronic features of bridged ligands and their semiconducting properties. The study of the electronic structure of this family of compounds may help to rationalize the effects of several factors in the conducting properties of these materials.

To answer these and others questions, we study the electronic structure of the complexes and the polymers of ruthenium, respectively. Figs. 1–3 show the phthalocyanoruthenium complex, the polymers, and the bridged ligands, respectively.

2. Calculations

We used the Amsterdam Density Functional [26,27] (ADF 2.3 version) program package, based on the LCAO density functional for the complexes and polymers (ADF-band 1.0 version) [28]. Bonding energies were evaluated by the generalized transition-state method. We have included Becke's nonlocal

correction [29] to the local HFS exchange energy (local density approximation LDA) as well as Stoll's correction [30] for correlation between electrons of different spins, based on Vosko et al. parametrization [31] from electron gas data.

Moreover, for the calculation on the polymers, we have used the ADF band code at the LDA level of theory and nonlocal gradient corrections by Becke for the exchange energy. All the calculations were performed with an integration accuracy greater than 10^{-4} and at 10 k-points in the reduced Brillouin zone for all the one-dimension (1D) cells.

The molecular orbitals were expanded in an uncontracted double- ξ STO basis set [32] for all atoms with the exception of the transition metal (Ru) orbitals, for which we used a triple- ξ basis set. As polarization functions one 5p STO were used for Ru. The cores (Ru: 1s–3d; C, N = 1s) were kept frozen [26,27]. For the polymers, we have used a basis set of numerical atomic orbital (NAOs) obtained from the STOs for each atom.

In order to analyze the interactions between [PcRu] and two bridged ligand molecules (L) in the complexes, we decomposed the bonding energy into a number of terms, using the scheme of Morokuma [33]. The binding energy, ΔE , is obtained from the difference between the complex and the fragments:

$$\Delta E = E^{\text{PcRu(L)}_2} - E^{\text{PcRu}} - E^{(\text{L})_2} \quad (1)$$

The binding energy can be decomposed in two terms,

$$\Delta E = \Delta E^0 + \Delta E_{\text{oi}} \quad (2)$$

The first term, ΔE^0 , is called the steric repulsion [34,35], which may be splitted at the same time into two components: (i) the electrostatic interaction ΔE_{elstat} of the nuclear charges and unmodified electronic-charge density of one fragment with those of the other fragment. Both fragments being at their final positions. Usually ΔE_{elstat} is negative, i.e. stabilizing. (ii) The other component is the exchange repulsion or Pauli repulsion ΔE_{pauli} [36,37]. This is due to the anti-symmetric requirement of the total wavefunction. It could be understood in a one-electron model as arising from the two-orbital four- (three-) electron destabilizing interactions between occupied orbitals on the fragments. The steric repulsion term ΔE^0 is usually repulsive at the equilibrium distance, since the repulsive component ΔE_{pauli} dominates in that region.

The second term, ΔE_{oi} comes from the mixing of virtual orbitals of the fragments with the occupied orbitals. This is called the electronic interaction energy [38].

On the other hand, we are interested in estimating the band gap of these systems. In the context of density functional theory (DFT) the energy gap is twice the hardness η [39,40]. This last quantity is defined as [41],

$$\eta = \frac{1}{2} \left(\frac{\partial^2 E}{\partial N^2} \right)_{\nu} \cong \frac{(I - A)}{2} \quad (3)$$

where E is the electronic energy; N , the number of electrons; ν , the external potential; I , the ionization potential; and A , the electron affinity. Working definitions of the quantities I and A are possible within molecular theory [42,43]. According to Koopmans's theorem, the ionization potential and electron affinity may be approximated in the molecular orbital theory

as $I \cong -\epsilon_{\text{HOMO}}$ and $A \cong -\epsilon_{\text{LUMO}}$ [44], respectively. With these approximations, the hardness is just half the energy gap between the highest occupied molecular orbital (HOMO) and the lowest unoccupied molecular orbital (LUMO),

$$\eta \cong \frac{\epsilon_{\text{LUMO}} - \epsilon_{\text{HOMO}}}{2} \quad (4)$$

A bigger η means a large I and a smaller A , which implies that the system has a smaller tendency to accept electrons and/or a smaller tendency to give away electrons. Thus, hardness can be seen as a resistance to charge transfer [39,40]. For solids, η is the half of the energy gap (ΔE gap) [39,40],

$$\eta = \frac{\Delta E_{\text{gap}}}{2} \quad (5)$$

The conductivity (σ) of a semiconductor depend on the energy required to promote electrons from the Fermi level across the band gap (E_g) [45,46]. Therefore, we qualitatively associate the magnitude of η and energy gap with the property of semiconductivity in the systems under study [43]. Thus, we will have an approximated index to compare and to explain the experimental values as conductivity and band gap.

We have first performed calculations on [PcRu] isolated molecule using the experimental geometry (X-ray data) [47], with appropriate averaging of bond angles and bond lengths to maintain the D_{4h} symmetry. The coordinate system used in the calculation is shown in Fig. 1. The monomers have been built by linking [PcRu] (metallomacrocyclole) with linear bidentate bridging ligands, metal over ligand, along the stacking direction (z axis in our coordinate system). In the Fig. 2 is shown the molecular stack. We have used the bridging ligands: pyrazine (pyz), triazine (tri), tetrazine (tz), 4,4'-bipyridine (byp), bipyridylacetylene (byac) (see Fig. 3). The bridged structure shown in Fig. 2 has been confirmed for many compounds using a variety of physical methods (IR, mössbauer spectroscopy, NMR, thermogravimetry, and scanning tunneling microscopy) [1–10,48,49].

We have used experimental geometry of [PcRu] in the monomers and polymers. Furthermore, we take the distance Ru–N (bridged ligands) at 2.5 Å, according to experimental data by X-ray absorption spectroscopy [50,51]. We have optimized the geometry of the

Table 1
Percent contribution of Pc and Ru fragments to selected orbitals (based on Mulliken Population Analysis per MO) of phthalocyanoruthenium, where only the main contributions to each orbital have been given

ϵ (eV)	Occupation	Ru	Pc
$13a_{1g}^{\beta}$ -4.282	0	84 (d_{z^2} , 5s)	16
$6e_{1g}^{\beta}$ -4.708	0	66 ($d\pi$)	34
$6b_{2g}^{\beta}$ -5.079	1	82 (d_{xy})	18
$2a_{1u}^{\alpha}$ -5.219	1	0	100
$2a_{1u}^{\beta}$ -5.524	1	0	100
$9b_{2g}^{\alpha}$ -6.666	1	55 (d_{xy})	45
$6e_{1g}^{\alpha}$ -6.670	1	51 ($d\pi$)	49
$13a_{1g}^{\alpha}$ -6.834	1	88 (d_{z^2})	12

bridged ligands, using the ADF code. The resulting geometries are used in the calculations of monomers and polymers.

3. Results and discussion

3.1. [PcRu(L₂)] complexes

3.1.1. Orbital interactions

We performed a fragmentation analysis on [PcRu(L)]_n polymers (L = pyz, tri, tz, bpy, bpyac) from their respective monomers. Building up stepwise these models, the molecular approach should depict the frontier orbitals implicated in the valence (highest occupied) and conduction (lowest unoccupied) bands. We analyzed the electronic structure of the [PcRu(L)₂] complexes. However, before describing the metal-bridged ligand interaction, it is necessary to show the changes that occur when the Ru(II) is inserted in the phthalocyanine macrocycle, Pc⁻².

Table 2
Energetic barrier ($\Delta E_{\text{barrier}}$, Kcal/mol) upon variation of the rotation angle of the axial ligand from 0 to 45°

Complex	$\Delta E_{\text{barrier}}$ (Kcal/mol)
[PcRu(pyz ₂)]	-10.36
[PcRu(tri ₂)]	-10.22
[PcRu(tz ₂)]	-8.461
[PcRu(bpy ₂)]	-9.526
[PcRu(bpyac ₂)]	-9.284

The [PcRu] fragment has D_{4h} symmetry. Table 1 shows the one-electron levels obtained by unrestricted calculations for the metallomacrocyclic. The ground states of [PcRu] is 3E_g with two electrons unpaired. For a discussion of the trends in the one-electron energies, it is instructive to look at the composition of the individual orbitals. In Table 1 the composition of the most important orbitals are given in terms of Ru and Pc orbitals.

We have found that the increasing energy level order of the metal orbitals are $d_{x^2-y^2} > d_{xy} > d\pi(d_{xz}, d_{yz}) > d_{z^2}$. The level $2a_{1u}$ of the Pc⁻² is found in the frontier region between d_{xy} and $d\pi$ metal orbitals. The electronic ground-state configuration (d_{xy})² ($d\pi$)³ (d_{z^2})¹ is the same given from phthalocyanoiron [15], where a double occupation for d_{xy} is suggested. The LUMO is $13A_{1g}^{\beta}$. The LUMO + 1 orbitals, $7e_g(\pi^*)$, comes from an interaction between $d\pi$ of metal and $6e_g(\pi^*)$ of the Pc⁻², not shown here.

The fragmentation analysis was performed in order to know what happens when the metalomacrocyclic [PcRu] is connected with the bridged ligands. The introduction of axial ligands modifies the Phthalocyanoruthenium (PcRu) ground-state electronic configuration described above. Experimental evidence confirm a low spin pseudo-octahedral Ru(II) environment in [PcRu(L₂)] complexes as well as [PcRu(L)]_n polymers [52–56]. Furthermore, these compounds show an ESR silent sign, associated with a restricted electronic state [3,5]. We have used this electronic state for studying the [PcRu(L₂)] complexes with L = pyz, tri, tz, bpy, and bpyac.

We found that in all the studied complexes, axial ligand prefer to be located towards the aza nitrogen atoms of [PcRu]. Table 2 shows the energy barrier that exists when the bridged ligands go from a position pointing to the pyrrolic nitrogenous (N_p, 0°) towards the position pointing to the aza nitrogenous (N_a, 45°). In the Section 3.1.2, we will try to find an explanation to this result.

In Fig. 4, the ground-state one-electron levels are shown for the series [PcRu(L₂)] with L = pyz, tri, tz, bpy, and bpyac. For some selected complexes and their molecular orbitals, an atomic orbital population analysis is given in Table 3. The monomers show different symmetry labels: [PcRu(L₂)] where pyz, bpy, and bpyac have a C_{2h} symmetry. For L = tri and tz, the symmetry became C_{2v} . For brevity, we

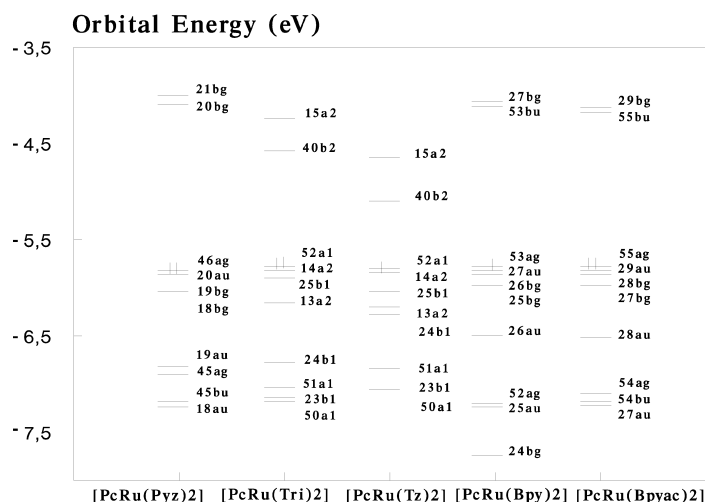


Fig. 4. Energy level frontier for the $[\text{PcRu}(\text{L}_2)]$ complexes with $\text{L} = \text{pyz}, \text{tri}, \text{tz}, \text{bpy}, \text{bpyac}$. All lower lying orbitals are also doubly occupied.

will describe the frontier orbital of monomers $[\text{PcRu}(\text{L}_2)]$ with $\text{L} = \text{pyz}$ and tz . This is due to the fact that the results of pyz are similar to that obtained with bpy and bpyac . On the other hand, the results of tz are similar to that obtained with tri .

As it is expected for phthalocyanoruthenium, the d_{z^2} orbital is highly destabilized though the sigma interaction with the HOMO of the bridged ligands. The d_{z^2} orbital remains empty. Furthermore, the π -donation destabilization of the $d(\pi)$ orbitals (d_{xz} and d_{yz}), even

Table 3

Percentage contribution of individual fragments to selected orbitals (based on Mulliken Population Analysis per MO) of $[\text{PcRu}(\text{L}_2)]$ with $\text{L} = \text{pyz}, \text{tri}, \text{tz}, \text{bpy},$ and bpyac

$[\text{PcRu}(\text{pyz}_2)] \epsilon$ (eV)	-4.02	-4.10	-5.82(HOMO)	-5.84	-5.88	-6.07	-6.81
Orbital symmetry	$21b_g$	$20b_g$	$46a_g$	$20a_u$	$19b_g$	$18b_g$	$19a_u$
Ru	11.7	0.00	79.7(d_{xy})	0.00	61.8(d_{yz})	53.2(d_{xz})	0.00
Pc	67.2	72.5	20.3	100	38.2	46.8	0.00
Pyz	21.1	27.5	0.00	0.00	0.00	0.00	100
$[\text{PcRu}(\text{tri}_2)] \epsilon$ (eV)	-4.23	-4.58	-5.78(HOMO)	-5.80	-5.89	-6.17	-6.76
Orbital symmetry	$15a_2$	$40b_2$	$52a_1$	$14a_2$	$25b_1$	$13a_2$	$24b_1$
Ru	0.00	0.00	77.4(d_{xy})	0.00	52.0(d_{yz})	53.7(d_{xz})	0.00
Pc	49.3	0.00	22.6	100	47.9	38.3	0.00
Tri	50.7	100	0.00	0.00	0.00	8.10	100
$[\text{PcRu}(\text{tz}_2)] \epsilon$ (eV)	-4.65	-5.09	-5.79(HOMO)	-5.80	-5.84	-6.05	-6.21
Orbital symmetry	$15a_2$	$40b_2$	$52a_1$	$14a_2$	$25b_1$	$24b_1$	$13a_2$
Ru	9.19	0.00	75.5(d_{xy})	00.0	49.1(d_{yz})	9.31	51.2(d_{xz})
Pc	0.00	0.00	24.5	100	37.6	90.7	40.2
Tz	90.8	100	0.00	0.00	13.3	0.00	8.60
$[\text{PcRu}(\text{bpy}_2)] \epsilon$ (eV)	-4.07	-4.09	-5.77(HOMO)	-5.82	-5.85	-5.97	-6.50
Orbital symmetry	$27b_g$	$53b_u$	$53a_g$	$27a_u$	$26b_g$	$25b_g$	$26a_u$
Ru	10.3	0.00	81.9(d_{xy})	0.00	62.9(d_{yz})	55.7(d_{xz})	0.00
Pc	69.4	74.7	18.1	100	37.1	44.3	0.00
Bpy	20.3	25.3	0.00	0.00	0.00	0.00	100
$[\text{PcRu}(\text{bpyac}_2)] \epsilon$ (eV)	-4.11	-4.20	-5.77(HOMO)	-5.82	-5.85	-5.97	-6.51
Orbital symmetry	$29b_g$	$55b_u$	$55a_g$	$29a_u$	$28b_g$	$27b_g$	$28a_u$
Ru	11.2	0.00	82.4(d_{xy})	0.00	63.8(d_{yz})	0.00(d_{xz})	0.00
Pc	88.8	73.2	17.6	100	36.2	100	0.00
Bpyac	0.00	26.8	0.00	0.00	0.00	0.00	100

Table 4
Hardness results for [PcRu(L₂)] complexes. Energies in eV

Complex	LUMO	HOMO	η
[PcRu(py ₂) ₂]	−4.101	−5.824	0.862
[PcRu(tri ₂) ₂]	−4.581	−5.779	0.599
[PcRu(tz ₂) ₂]	−5.090	−5.789	0.350
[PcRu(bpy ₂) ₂]	−4.089	−5.769	0.840
[PcRu(bpyac ₂) ₂]	−4.189	−7.774	0.793

thought not as pronounced as that of the d_{z²} orbital, appears to be strong enough to increase the back-bonding from the metal to the LUMO, which has a high contribution from the macrocycle ring.

As mentioned before, the main interests of this paper resides in the electronic properties. Therefore, we analyzed the highest occupied molecular and the lowest unoccupied orbitals. In the monomers, the HOMO is a d_{xy} of transition metal. This orbital is practically fixed in energy for the set of axial ligands (see Fig. 4).

Respect to LUMO, when [PcRu(py₂)₂] monomer is formed, such orbital arises from the interaction between one metallomacrocycle π^* orbital and pyrazine ligand π^* orbital. Both with b_g symmetry. This interaction has no direct energetic consequences, since the bonding combination is unoccupied (20b_g). The LUMO orbital, 20b_g, shows the following composition: 72.5% from π^* system [PcRu] and 21.5% from π^* pyrazine ligand. In contrast, when the bridged ligand is tetrazine, the LUMO orbital in [PcRu(tz₂)₂] is 100% formed by π^* system of such ligand. This is a nonbonding orbital. However, the HOMO–LUMO gap is considerably

Table 6
Summary of results for (i) [PcRu(py₂)_n], (ii) [PcRu(tz)_n], (iii) [PcRu(py₂)₂], and (iv) [PcRu(tz₂)₂] (energy in eV)

	i ^a	ii ^a	iii	iv
HOMO ^b	−5.824	−5.789	−5.824	−5.789
LUMO ^c	−5.380	−5.658	−4.101	−5.090
Gap ^d	0.444	0.131	1.723	0.699

^a For polymers i and ii, the corresponding terms are HOCO, LUCO and band gap.

^b Highest occupied molecular orbital.

^c Lowest unoccupied molecular orbital.

^d Transition energy between the HOMO and the LUMO.

smaller than the system with pyz, when it is used as a bridging ligand. This description confirms the best semiconduction properties associated to the tetrazine as ligand. Similar results were found for the iron compounds [15].

We have calculated the hardness of the complexes studied from the Eq. (4). The results are summarized in Table 4. The smaller the hardness value, the better will be the semiconduction. Furthermore, when the number of nitrogen atoms in the axial ligand increases (for example pyz to tz), the semiconduction is enhanced. This is due to the fact that a nitrogen atom is more electronegative than the −CH group, producing a greater stabilization of the ligand's LUMO, and therefore a reduction in the HOMO–LUMO gap. The hardness in the systems of ruthenium is something greater than for those of iron. The difference is found in the energetic level of the HOMO, since in the compounds of ruthenium such orbital is most stabilized.

Table 5
Contributions (eV) to the bonding energy of [PcRu(L₂)] complexes

Complex	ϕ (°)	ΔE_{elstat}	ΔE_{Pauli}	ΔE°	ΔE_{io}	ΔE_{total}
[PcRu(py ₂) ₂]	0	−14.461	39.355	24.894	−33.102	−8.208
	45	−13.963	38.510	24.547	−33.204	−8.657
[PcRu(tri ₂) ₂]	0	−12.833	35.162	22.329	−30.763	−8.434
	45	−12.526	34.657	22.131	−31.009	−8.878
[PcRu(tz ₂) ₂]	0	−12.327	34.204	21.877	−30.433	−8.556
	45	−12.074	33.772	21.698	−30.620	−8.922
[PcRu(bpy ₂) ₂]	0	−15.064	38.777	23.713	−30.024	−6.311
	45	−14.555	38.035	23.480	−30.204	−6.724
[PcRu(bpyac ₂) ₂]	0	−15.069	38.765	23.696	−30.011	−6.315
	45	−14.555	38.011	23.456	−30.174	−6.718

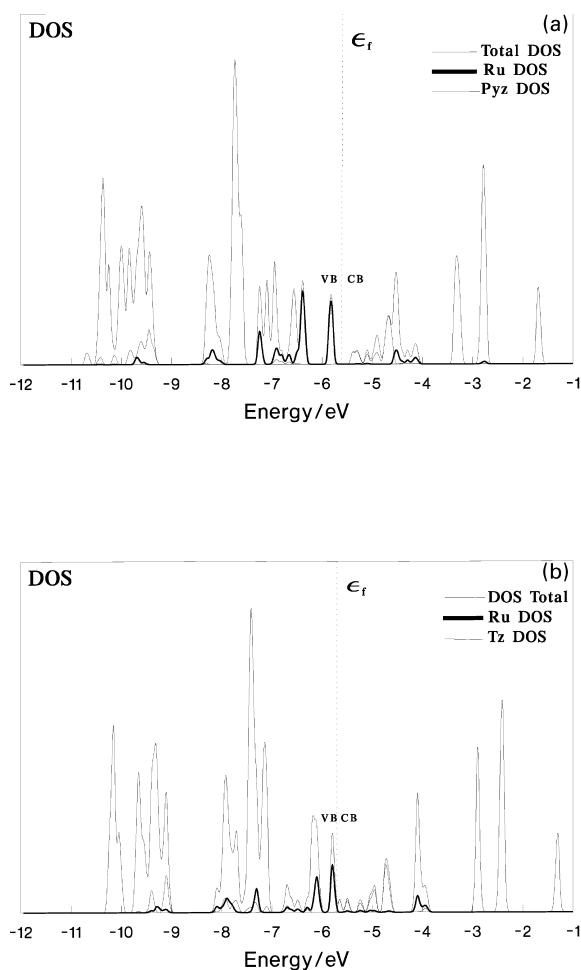


Fig. 5. Band structures for (a) $[\text{PcRu}(\text{pyz})]_n$ and (b) $[\text{PcRu}(\text{tz})]_n$.

3.1.2. Energy decomposition

We will try to explain why an axial ligand prefer to be located towards the aza nitrogen atoms of phthalocyanoruthenium. To achieve this, we decompose the bonding energy in the rotation of the ligand from 0 to 45° (conformation more stable) keeping the Ru–N (ligand) distance fixed at 2.5 Å. It should be noted that most of these interactions involve orbitals and have been referred in the calculation as four-electron two-orbital repulsion. The results of this analysis are shown in Table 5. According to the data reported in the third column of Table 5, a rotation of 45° of the axial ligands induces in the complex series a decrease in the attractive electrostatic interaction ΔE_{elstat} . These can be explained since a 45° conformation increases the distances between most of the atoms of the two interacting fragments, in such a way that the stabilizing interactions between the charge density of one fragment with the nuclei of the other fragment decreases. Looking at the Pauli repulsion term, ΔE_{Pauli} , is reduced, upon variation of the rotation angle from 0 to 45°. This could be understood in terms of a decrease of the overlap between most of the occupied orbitals on the interacting fragments. The Pauli repulsion term is highly positive in all the complexes. It should be noted that although the Pauli repulsion decreases when the axial ligands are in a conformation of 45°, it still remains strong.

ΔE_{Pauli} and ΔE_{elstat} change in apposite directions upon changing the rotation angle, but ΔE_{Pauli} is larger in absolute terms and has a larger variation. Thus, when ΔE_{Pauli} and ΔE_{elstat} are combined into the steric interaction energy (ΔE°) one finds that ΔE° is destabilizing (positive), both for the 0 and 45° configurations, but is smaller for that last. As far as the stabilizing orbital interaction term ΔE_{oi} is concerned,

Table 7

Summary of computational results for the $[\text{PcRu}(\text{L})]_n$ polymers. Experimental energy gaps and conductivity (σ , S/cm)[1–10]. (Energy in eV.)

Polymer	LUCO ^a	HOCO ^b	Band gap theoretical ^c	Band gap experimental	σ
$[\text{PcRu}(\text{pyz})]_n$	−5.380	−5.824	0.222		1×10^{-7}
$[\text{PcRu}(\text{tri})]_n$	−5.507	−5.779	0.136		7×10^{-4}
$[\text{PcRu}(\text{tz})]_n$	−5.658	−5.789	0.066	0.20	1×10^{-2}
$[\text{PcRu}(\text{bpy})]_n$	−4.750	−5.769	0.510		2×10^{-8}
$[\text{PcRu}(\text{bpyac})]_n$	−4.635	−5.774	0.570		1×10^{-9}

^a Lowest unoccupied crystal orbital.

^b Highest occupied crystal orbital.

^c Transition energy between the HOCO and the LUCO.

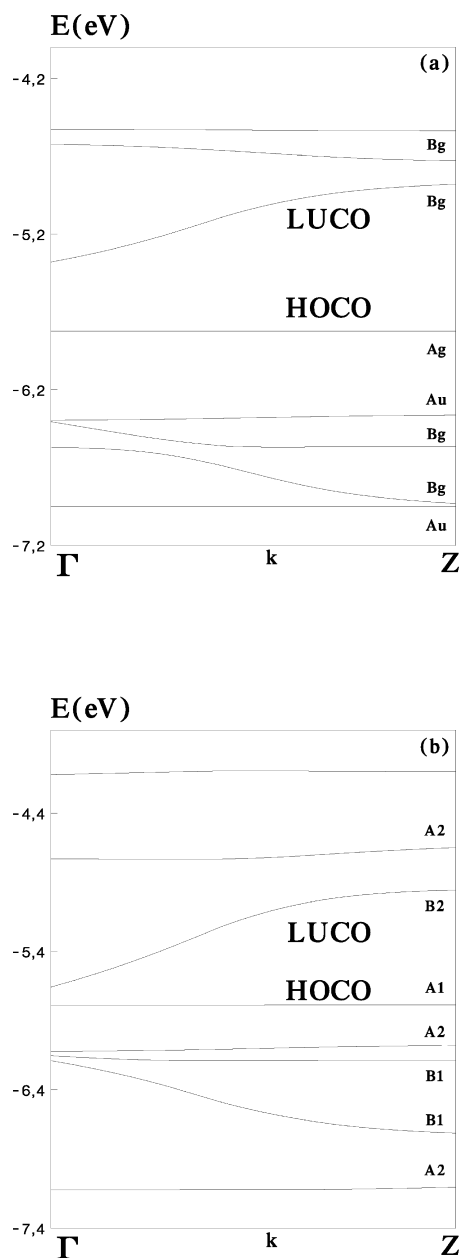


Fig. 6. Density of states for $[\text{PcRu}(\text{L})]_n$ polymers with the projections Ru, pyz, and tz, which illustrate the nature of the frontier crystal orbital: (a) $[\text{PcRu}(\text{pyz})]_n$ and (b) $[\text{PcRu}(\text{tz})]_n$.

we first notice that it is little influenced upon the variation of axial ligands, and secondly, it gives the stabilizing contribution for each conformation, but it is rather insensitive to the change of the ligand groups.

From Table 5, it can be appreciated that the steric repulsion dominates over the attractive occupied/virtual orbital interaction upon variation of the rotation angle from 0 to 45°. We have therefore clearly identified the Pauli repulsion as the origin of the configuration at 45° with respect to the axial ligands as the more stable conformation.

3.2. $[\text{PcRu}(\text{L})]_n$ polymers

When going from the complex to the infinite chain, due to the stacked effects of $[\text{PcRu}]$ units, we would have to expect a smaller band gap. We used pyz and tz as models. Table 6 shows such effect for the systems with pyz and tz in dimers and polymers, respectively. The band gap is reduced upon the formation of the polymer.

We have described the frontier band structures for the $[\text{PcRu}(\text{L})]_n$ with $\text{L} = \text{pyz}, \text{tz}$. Thereafter, we will make a generalization of the results found for the rest of the polymers. Only the highest occupied frontier crystal orbitals (HOCOs) and the two lowest unoccupied CO (LUCOs) are shown in the range -7.2 – -4.1 eV in Fig. 5(a) and (b). There are several flat bands, which correspond to well localize electrons. For simplicity, we continue using the symmetry of the complexes in the polymers. Among them, we found that the bands fall in the -7.2 – -5.5 eV range, which is associated to the highest occupied crystal orbital (HOCO) corresponding to d_{xy} and the π -bands of the Ru atom. Besides, we have found in this range a band with a quite dispersed, a_g and a_1 symmetry corresponding to Pc in the $[\text{PcRu}(\text{pyz})]_n$ and $[\text{PcRu}(\text{tz})]_n$ polymers, respectively.

A different situation is appreciated in the conduction band corresponding to the LUCO. Let's write out the Bloch functions at the center ($k = 0, \Gamma$) and edge ($k = \pi/a, Z$) of the Brillouin zone. The LUCO band for the polymers runs up towards Z vector, which in turn corresponds to the most antibonding combination. The composition of this band is very similar to that shown by the monomer. Thus, the polymer with pyz shows a composition which is 70% PcFe and a 30% bridging ligand; while with tz, the composition is 100% formed by π^* system of such ligand.

In Table 7, we have summarized the results for all polymers including experimental measures [1–10]. The metallomacrocyclic polymers with bridged

ligands, showed semiconducting properties, in agreement with the experimental measurements of conductivity. It is interesting to note that the theoretical band gap by $[\text{PcRu}(\text{tz})]_n$ polymer agrees with the experiment.

We have also built the density of states (DOS) [57,58] and its projection on the Ru and bridged ligands. The DOS show the behaviors described in the band structures for the $[\text{PcRu}(\text{L})]_n$ ($\text{L} = \text{pyz}, \text{tz}$) systems (Fig. 6). The projections of the metal and bridged ligand orbitals in the density of states showed mainly a metal character in the valence band (VB) near the Fermi level, and the ligand participation in the conduction band (CB). Independent of the polymer, both the HOCO and LUCO bands are very similar to those of the monomeric units described previously.

4. Conclusions

The analysis of the electronic structures of the polymers and complexes indicate that: (i) the HOCO is a very flat band, largely composed of the transition metal orbitals (approximately 80%). (ii) The LUCO band is composed of a mixture between the ring and bridged ligand orbitals, as in the case of the systems formed by pyz, bpy, and bpyac. This composition is different by polymers formed with tri and tz. Such a band is exclusively composed of the π system of tri and tz. Thus, these systems showed the highest conductivity of the polymer studied here.

Acknowledgements

This work was supported by the FONDECYT Project No. 1990038. Also, the author thank Dr Luis Padilla (Comisión Chilena de Energía Nuclear) for the access to the ADF 2.3 version package.

References

- [1] G.E. Kellogg, J.G. Gaudiello, Polymeric coordination complexes: bridging molecular metals and conductive polymers, in: D.W. Bruce, D. O'Hare (Eds.), *Inorganic Materials*, Wiley, New York, 1992, pp. 353–404.
- [2] S. Deger, A. Lange, M. Hanack, *Chem. Coord. Rev.* 83 (1988) 115.
- [3] H. Schultz, H. Lehmann, M. Rein, M. Hanack, *Struct. Bonding* 74 (1991) 41.
- [4] M. Hanack, *Macromol. Symp.* 80 (1994) 83.
- [5] M. Hanack, M. Lang, *Adv. Mater.* 6 (1994) 819.
- [6] C.-T. Chen, K.S. Suslick, *Coord. Chem. Rev.* 128 (1993) 193.
- [7] M. Hanack, S. Knecht, M. Schulte, *J. Organometall. Chem.* 445 (1993) 157.
- [8] S. Knecht, R. Polley, *Chem. Ber.* 128 (1995) 928.
- [9] J. Pohmer, M. Hanack, J. Barcina, *J. Mater. Chem.* 6 (1996) 957.
- [10] Y.G. Kang, H. Kim, *Synth. Met.* 78 (1997) 11.
- [11] H.-H. Wang, J.M. Williams, M.-H. Whangbo, *Synth. Met.* 41 (1991) 1983.
- [12] M.-H. Whangbo, K.R. Stewart, *Isr. J. Chem.* 23 (1983) 133.
- [13] E. Canadell, S. Alvarez, *Inorg. Chem.* 23 (1984) 573.
- [14] F. Mendizabal, C. Olea-Azar, G. Zapata-Torres, F. Eisner, *Theochem* 534 (2001) 23.
- [15] F. Mendizabal, C. Olea-Azar, R. Briones, *Int. J. Quantum Chem.* 82 (2001) 170.
- [16] M. Hanack, S. Gül, L.R. Subramanian, *Inorg. Chem.* 31 (1992) 1542.
- [17] U. Keppler, S. Deger, A. Lange, M. Hanack, *Angew. Chem. Int. Ed. Engl.* 26 (1987) 724.
- [18] B.N. Diel, T. Inabe, N.K. Jaggi, J.W. Lyding, O. Schneider, M. Hanack, C.R. Kannewurf, T.J. Marks, L.H. Schwartz, *J. Am. Chem. Soc.* 106 (1984) 3207.
- [19] J. Kleinwächter, M. Hanack, *J. Am. Chem. Soc.* 119 (1997) 10684.
- [20] J.G. Gaudillo, G.E. Kellogg, S.M. Tetrick, T.J. Marks, *J. Am. Chem. Soc.* 111 (1989) 5259.
- [21] M. Hanack, U. Schlick, *Inorg. Chem.* 34 (1995) 3621.
- [22] O. Schneider, M. Hanack, *Chem. Ber.* 116 (1983) 2088.
- [23] H. Meier, W. Albrecht, E. Zimmerhackl, M. Hanack, J. Metz, *J. Synth. Met.* 11 (1985) 333.
- [24] H. Meier, W. Albrecht, M. Hanack, J. Koch, *Polym. Bull.* 16 (1986) 75.
- [25] C.F. van Nostrum, R.J. Nolte, *Chem. Commun.* (1996) 2385.
- [26] E.J. Baerends, D.E. Ellis, P. Ros, *Chem. Phys.* 2 (1973) 42.
- [27] E.J. Baerends, P. Ros, *Int. J. Quantum Chem.* S12 (1978) 169.
- [28] G. te Velde, E.J. Baerends, *Phys. Rev.* 44B (1991) 7888.
- [29] A.D. Becke, *J. Chem. Phys.* 84 (1986) 4524.
- [30] H. Stoll, E. Golka, E. Preuss, *Theor. Chim. Acta* 29 (1980) 55.
- [31] S.H. Vosko, L. Wilk, M. Nusair, *J. Can. J. Phys.* 58 (1980) 1200.
- [32] J.G. Snijders, P. Vernooijs, E.J. Baerends, *At. Data Nucl. Data Tables* 26 (1982) 483.
- [33] K. Morokuma, *Acc. Chem. Res.* 10 (1977) 294.
- [34] T. Ziegler, A. Rauk, *Inorg. Chem.* 18 (1979) 1558.
- [35] T. Ziegler, A. Rauk, *Inorg. Chem.* 18 (1979) 1755.
- [36] H. Fujimoto, J. Osamura, T. Minato, *J. Am. Chem. Soc.* 100 (1978) 2954.
- [37] K. Kitaura, K. Morokuma, *Int. J. Quantum Chem.* 10 (1976) 325.
- [38] T. Ziegler, A. Rauk, *Theor. Chim. Acta* 46 (1977) 1.
- [39] R.G. Parr, W. Yang, *Density Functional Theory of Atoms and Molecules*, Oxford University Press, New York, 1989.
- [40] W. Kohn, A.D. Becke, R. Parr, *J. Phys. Chem.* 100 (1996) 12974.

- [41] R.G. Parr, R.A. Donnelly, M. Levy, W.E. Palke, *J. Chem. Phys.* 68 (1978) 3801.
- [42] R.G. Pearson, *Acc. Chem. Res.* 26 (1993) 250.
- [43] R.G. Pearson, *Chemical Hardness*, Wiley-VCH Verlag GmbH, New York, 1997.
- [44] T.A. Koopman, *Physica* 1 (1933) 104.
- [45] F. Mendizabal, R. Contreras, A. Aizman, *Int. J. Quantum Chem.* 56 (1995) 820.
- [46] F. Mendizabal, R. Contreras, A. Aizman, *J. Phys.: Condens. Matter* 9 (1997) 3011.
- [47] H. Bertagnolli, A. Weber, W. Hörner, T. Ertel, U. Reinöhl, *Inorg. Chem.* 36 (1997) 6397.
- [48] J. Metz, O. Schneider, M. Hanack, *Spectrochim. Acta* (1982) 1265.
- [49] M. Hanack, U. Keppeler, M. Lange, A. irsch, R. Dieing, in: C.C. Leznoff, A.B.P. Lever (Eds.), *Phthalocyanines, Properties and Applications*, vol. 2, VCH, Weinheim, 1993.
- [50] L. Alagna, A. Capobianchi, P. Marovino, A.M. Paoletti, G. Pennesi, T. Prospero, G. Rossi, *Inorg. Chem.* 38 (1999) 3688.
- [51] G. Rossi, M. Gardini, G. Pennesi, C. Ercolani, V.L. Goedken, *J. Chem. Soc., Dalton Trans.* (1989) 193.
- [52] U. Keppeler, W. Kobel, H.-U. Siehl, M. Hanack, *Chem. Ber.* 118 (1985) 2095.
- [53] R. Aldinger, M. Hanack, K. Herrmann, A. Hirsch, K. Kasper, *Synth. Met.* 60 (1993) 265.
- [54] M. Hanack, M. Mezger, W. Hiller, *Acta Crystallogr.* 43C (1987) 1264.
- [55] C.C. Leznoff, A.B.P. Lever, *Phthalocyanines-Properties and Applications*, vols. 1–4, VCH, New York, 1986.
- [56] A. Capobianchi, A.M. Paoletti, G. Pennesi, G. Rossi, R. Caminiti, C. Ercolani, *Inorg. Chem.* 33 (1994) 4635.
- [57] H.L. Yu, *Phys. Rev.* 15B (1977) 3609.
- [58] R. Arratia-Perez, *Chem. Phys. Lett.* 213 (1993) 547.